

Research Article

Abdul Kareem M. B. Al-Shammaa* and A. T. Alisawi

Novel graph for an appropriate cross section and length for cantilever RC beams

<https://doi.org/10.1515/eng-2022-0428>

received October 28, 2022; accepted March 11, 2023

Abstract: Whether the design is done manually or by software, the designer will have difficulty choosing the economic and strength cross section. The designer, in this case, either relies on their experience or resorts to the method of trial and error. Especially for Cantilever beams with a long span as a result of risk deflections, it is exposed. The current theoretical study was performed on rectangular concrete cross sections of different dimensions and subjected to uniformly distributed loads. Based on a previous study, the sections are reinforced with a specific reinforcement ratio. Through an algorithm, Python 3.4 software, and an output file, the permissible deflections for each cross section were calculated according to the ACI 318M-19. Finally, the authors could draw a graph to choose the appropriate cross section for each required beam length in less time and effort.

Keywords: beam design, beam stiffness, sustained deflection, immediate deflection, beam deflection, cantilever beams

Notation

| | |
|---------|--|
| b | width of beam sections (mm) |
| d | adequate depth of beam sections (mm) |
| h | total depth of beam sections (mm) |
| ρ | reinforcement ratio in tension equal to (p) at output file. |
| ρ' | reinforcement ratio in compression. |
| A_s | steel area in tension (mm ²). |
| A_s' | steel area in compression (mm ²). |
| ℓ | span length of the beam and equal to (L) at output file (mm) |
| f_c' | ultimate compressive strength of concrete (MPa) |

| | |
|--------------------|---|
| E_s | modulus of elasticity for steel (MPa) |
| E_c | modulus of elasticity for concrete (MPa) |
| n | modular ratio of elasticity. |
| I_g | gross moment of inertia for beam sections (mm ⁴) |
| I_e | effective moment of inertia (mm ⁴) |
| I_{cr} | cracking moment of inertia (mm ⁴) |
| M_n | nominal bending moment (kN m) |
| M_{cr} | cracking moment (kN m) |
| M_a | maximum bending moment (kN m) |
| IDL | initial dead loads without self-weight (kN) |
| W_{LL} | unfactored live loads (kN) |
| W_{DL} | unfactored dead loads (kN) |
| Δ_{DL} | deflection due to dead load (mm) |
| $(\Delta_i)_{LL}$ | immediate deflection due to live load and equal to (Δ_i) at output file (mm) |
| $\Delta_{(DL+LL)}$ | deflection due to live plus dead loads (mm) |
| $\Delta_{(cr+sh)}$ | deflection due to creep and shrinkage of concrete (mm) |
| Δ_T | sustained deflection and equal to (Δ_T) at output file (mm) |
| γ | factor equal to $\frac{M_n}{bd^2}$, and equal to (y) at the output file (MPa) |

1 Introduction

Rectangular cross sections for concrete beams are commonly used to design reinforced concrete structures. While the design is done manually or by software, selecting the economical and strength cross sections for those beams is necessary. With the large-span cantilever beams, the selection is not easy and depends on the designer's experience with trial and error. The risk associated with the cross-sectional design becomes more severe for cantilever beams usually subjected to significant deflections. In Iraq, the construction of cantilever beams with rectangular sections appears in many hotels and commercial buildings. However, the authors did not find articles that studied the problem in detail.

What is specified at the ACI 318M-19 item 24.2 with SI unit [1] was performed to calculate the deflection. Nilson *et al.* [2] presented a graph shown in Figure 1, which is

* **Corresponding author: Abdul Kareem M. B. Al-Shammaa**, Department of Urban Planning, Faculty of Physical Planning, University of Kufa, Najaf, Iraq, e-mail: abdulkareem.baqir@uokufa.edu.iq
A. T. Alisawi: Department of Urban Planning, Faculty of Physical Planning, University of Kufa, Najaf, Iraq

essential to preparing the current study. From the group of curves, the common curve 60/4 was chosen, i.e., $f'_c = 4 \text{ ksi} = 28 \text{ MPa}$ and $f_y = 60 \text{ ksi} = 414 \text{ MPa}$. Nelson *et al.* [2–7] authored textbooks that contain chapters on deflection and how to calculate it. Metwally [8] confirmed that the support location affects the immediate deflection values. Chaphalkar *et al.* [9] emphasized that modeling can be made to analyze the deflection of cantilever beams by finite element package. Marovic *et al.* [10] concluded several models for calculating the deflection of the cantilever beams with end-concentrated loads with circular and hollow cross sections. The types of deflections are most important in checking the dimensions of the selected cross sections [11–23].

The current study aims to create a relationship between rectangular cross sections and the span lengths of reinforced concrete cantilever beams. Finally, the authors define the form of this relationship through a graph that facilitates the selection of strength and economic cross sections.

2 Design procedure

2.1 Assumptions

- In the tension zone, all sections are reinforced with a variable reinforcement ratio, while the compression zone is reinforced

with a minimum reinforcement content of ($\rho' = 0.002$). For the calculation of I_{cr} , the effect of compression steel has been neglected due to its proximity to the neutral axis and small quantity.

- The initial dead and live unfactored loads applied to the cantilever beams are calculated as follows:

Due to the thick slab: $0.15 \text{ m} = 0.15(25) = 3.75 \text{ kN/m}^2$,

Due to the thick sand: $0.05 \text{ m} = 0.05(17) = 0.85 \text{ kN/m}^2$,

Due to the thick flooring layers: $0.025 \text{ m} = (20 + 24)(0.025) = 1.1 \text{ kN/m}^2$.

Thus, initial dead loads (IDLs) = 5.70 kN/m^2 , while live load (W_{LL}) considered equal to 3 kN/m^2 . Usually, the lengths of adjacent slabs range from 4 to 5 m. Using an average of 4.5 m yields:

$IDL = 5.7(4.5) = 25.65 \text{ kN/m}$, $W_{LL} = 3(4.5) = 13.5 \text{ kN/m}$. By observing the constructed buildings in Iraq, these load values represent the worst case of loading excluding the concentrated loads.

- The approximate load values (if any) do not significantly affect the accuracy of the deflection results. The deflection of any structure depends mainly on the span length; as a result, the length is raised to the fourth power, while the load is to the first power. For example, the deflection of the cantilever beam due to the dead load is expressed as follows:

$$\Delta_{DL} = \frac{W_{DL}l^4}{8E_cI_{e1}}. \quad (1)$$

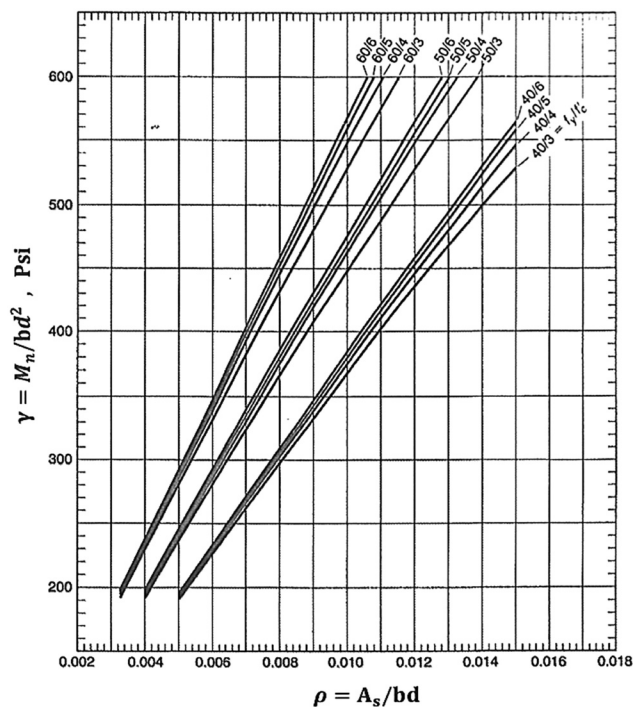


Figure 1: Strength of rectangular sections.

Table 1: Dimensions of the proposed cross sections

| γ (MPa) | ρ | h (mm) | γ (MPa) | ρ | h (mm) | γ (MPa) | ρ | h (mm) | γ (MPa) | ρ | h (mm) | γ (MPa) | ρ | h (mm) | γ (MPa) | ρ | h (mm) |
|----------------|--------|----------|----------------|--------|----------|----------------|--------|----------|----------------|--------|----------|----------------|--------|----------|----------------|--------|----------|
| 1.38 (200 psi) | 0.0034 | 500 | 2.76 (400 psi) | 0.0072 | 450 | 4.14 (600 psi) | 0.0110 | 400 | 4.83 (700 psi) | 0.0130 | 350 | 5.52 (800 psi) | 0.0150 | 300 | 5.52 (800 psi) | 0.0150 | 200 |
| | | 625 | | | 563 | | | 500 | | | 438 | | | 375 | | | 250 |
| | | 750 | | | 675 | | | 600 | | | 525 | | | 450 | | | 300 |
| | | 875 | | | 788 | | | 700 | | | 613 | | | 525 | | | 350 |
| | | --- | | | --- | | | 800 | | | 700 | | | 600 | | | 400 |

- The Flange effect is not considered because it is in a tension zone.
- The current study does not include deep beams with more than 900 mm depth because their reinforcement is distributed according to ACI item 9.9.
- The reinforcement can be placed in one or two layers in the tension zone. The adequate depth is taken as $d = h - 60$.

2.2 Calculations

Table 1 presents typical values for cross sections bh with h taken as a percentage of b . The difference of ρ values provided to the cross sections depends on the fact that ρ is inversely proportional to the section area bh . From Figure 1, the values of $(\frac{M_n}{bd^2} = \gamma)$ will be obtained by dropping each ρ on the curve (60/4). So, the span length is expressed as follows:

$$\gamma = \frac{M_n}{bd^2} = \frac{W \ell^2 / 2}{bd^2}, \quad \ell = \sqrt{\frac{2\gamma bd^2}{W}}. \quad (2)$$

According to an algorithm shown in Figure 2, the authors attempted to calculate the deflection of selected cross sections. Initial calculations show that the deflection of reinforced sections with $\rho = 0.015, 0.013, 0.011, 0.0072$ do not match the permissible sustained deflection, as mentioned at ACI (Table 24.2.2). So, the attempt was repeated but with $\rho = 0.0034, 0.0040, 0.0050, 0.0060$ and $\gamma = 1.38, 1.65, 1.96, 2.38$, respectively. Appendix A presents the input file using Python 3.4 software according to the input file data shown in Table 2.

2.3 Analysis results

- ACI – Table 24.2.2 provides two permissible deflections that must be checked: immediate deflections equal to $(\ell/360)$ and sustained deflections equal to $(\ell/240)$. The calculated deflections listed in Appendix B have been checked with the permissible ones to know the pass lengths with their cross sections, as shown in Table 3. Finally, the cross-sectional selection against the required length was facilitated by the graphic relationship shown in Figure 3.
- Mainly, increasing the depth of the beam means increasing its rigidity and thus increasing the permissible length of the beam so that it does not exceed the specificity of deep beams.
- The best span length is obtained for beams with a width of 350 mm, after which increasing the width becomes

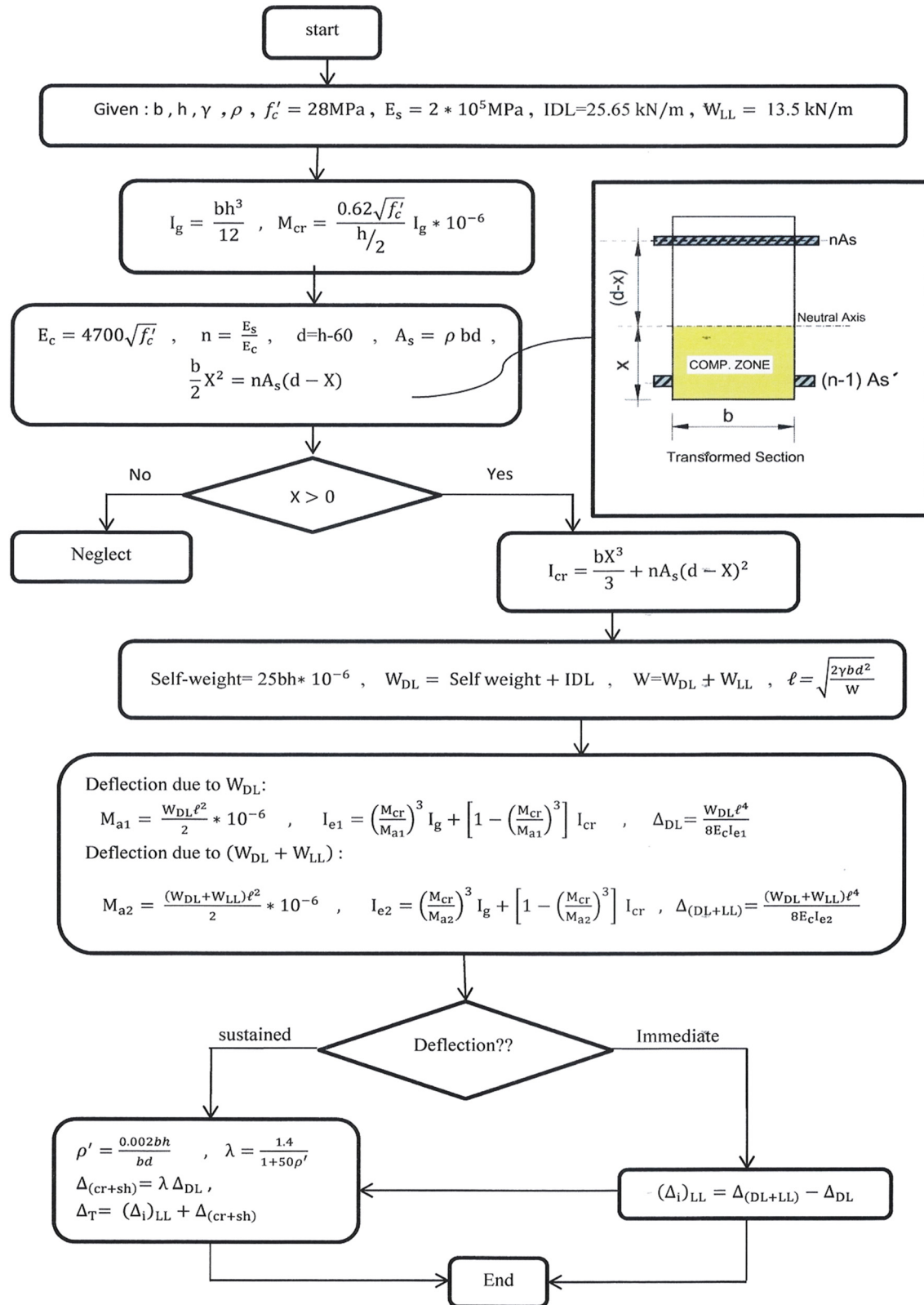


Figure 2: Flowchart to calculate beam deflections.

Table 2: Input file data

| γ (MPa) | | | | ρ | | | | h (mm) | | |
|----------------|----------------|----------------|----------------|--------|--------|--------|--------|----------|-----|----------|
| 2.38 (345 psi) | 1.96 (284 psi) | 1.65 (239 psi) | 1.38 (200 psi) | 0.0060 | 0.0050 | 0.0040 | 0.0034 | 375 | 250 | b (mm) |
| | | | | | | | | 500 | | |
| | | | | | | | | 563 | | |
| | | | | | | | | 625 | | |
| | | | | | | | | 450 | 300 | |
| | | | | | | | | 525 | | |
| | | | | | | | | 600 | | |
| | | | | | | | | 675 | | |
| | | | | | | | | 750 | | |
| | | | | | | | | 525 | 350 | |
| | | | | | | | | 613 | | |
| | | | | | | | | 700 | | |
| | | | | | | | | 788 | | |
| | | | | | | | | 875 | | |
| | | | | | | | | 600 | 400 | |
| | | | | | | | | 700 | | |
| | | | | | | | | 800 | | |

useless. An increase in a width greater than 350 mms means an increase in the weight of the beam at the expense of its rigidity.

- The sustained deflection is considered the most dangerous type, a discrepancy to what was believed in more detail in refs. [8,14,15,17,19]. All the empirical results in Appendix B agreed with the ACI conditions of immediate deflection, while sustained deflection is considered a criterion for

accepting pass results. For more explanation, an example can be taken from Appendix B, as shown in Table 4.

- Referring to the output file, it is noted that the allowable deflections for all sections were obtained from a trial ($\rho = 0.005$) against $\gamma = 1.96$ MPa. An increase in the reinforcement ratio of more than 0.005 gives an increase in length that does not meet ACI requirements. All deflections were calculated from unfactored loads based on the ACI conditions. However, the loads must be factored in when designing, and the reinforcement ratio will increase from 0.005, as shown in Appendix C. Increasing the reinforcement ratio provided that adhering to the length adopted in the current study means forming safer

Table 3: Check the results

| b (mm) | h (mm) | ℓ (mm) | Pass results (mm) | | ACI – provisions (mm) | |
|----------|----------|-------------|-------------------|------------|-----------------------|------------|
| | | | $(\Delta_i)_{LL}$ | Δ_T | $(\Delta_i)_{LL}$ | Δ_T |
| 250 | 375 | 1,530 | 2.25 | 4.704 | 4.25 | 6.37 |
| | 438 | 1,828 | 2.63 | 5.920 | 5.07 | 7.61 |
| | 500 | 2,118 | 2.96 | 7.074 | 5.88 | 8.82 |
| | 563 | 2,410 | 3.28 | 8.212 | 6.69 | 10.0 |
| | 625 | 2,695 | 3.57 | 9.304 | 7.48 | 11.2 |
| 300 | 450 | 2,050 | 3.15 | 7.289 | 5.69 | 8.54 |
| | 525 | 2,429 | 3.59 | 8.913 | 6.74 | 10.1 |
| | 600 | 2,802 | 4.00 | 10.47 | 7.78 | 11.6 |
| | 675 | 3,171 | 4.38 | 11.99 | 8.80 | 13.2 |
| | 750 | 3,536 | 4.74 | 13.45 | 9.82 | 14.7 |
| 350 | 525 | 2,604 | 4.06 | 10.26 | 7.23 | 10.8 |
| | 613 | 3,070 | 4.58 | 12.24 | 8.52 | 12.8 |
| | 700 | 3,523 | 5.05 | 14.31 | 9.78 | 14.6 |
| | 788 | 3,973 | 5.49 | 16.23 | 11.0 | 16.5 |
| | 875 | 4,412 | 5.88 | 18.06 | 12.2 | 18.4 |
| 400 | 600 | 2,919 | 4.46 | 10.07 | 8.10 | 12.1 |
| | 700 | 3,422 | 5.04 | 12.13 | 9.50 | 14.2 |
| | 800 | 3,915 | 5.55 | 14.10 | 10.8 | 16.3 |

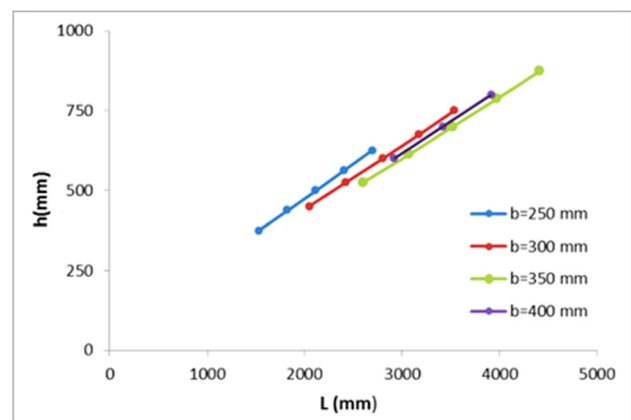


Figure 3: Optimum dimensions of R/C cantilever beams.

Table 4: Illustrative example

| b (mm) | h (mm) | ρ | γ (MPa) | ℓ (mm) | Empirical results (mm) | | ACI – provisions (mm) | |
|----------|----------|--------|----------------|-------------|------------------------|------------|-----------------------------|----------------------|
| | | | | | $(\Delta_i)_{LL}$ | Δ_T | $(\Delta_i)_{LL}(\ell/360)$ | $\Delta_T(\ell/240)$ |
| 250 | 375 | 0.0034 | 1.38 | 1,284 | 1.20 | 1.88 | O.K | O.K |
| 250 | 375 | 0.0040 | 1.65 | 1,404 | 1.82 | 3.22 | O.K | O.K |
| 250 | 375 | 0.0050 | 1.96 | 1,530 | 2.25 | 4.70 | O.K | O.K |
| 250 | 375 | 0.0060 | 2.38 | 1,686 | 2.72 | 6.82 | O.K | N.O.K |

Table 5: Empirical deflections due to overload

| Load increment % | Empirical results (mm) | | ACI – provisions (mm) | | Remark |
|------------------|------------------------|------------|-----------------------|------------|--------|
| | $(\Delta_i)_{LL}$ | Δ_T | $(\Delta_i)_{LL}$ | Δ_T | |
| 5.00 | 4.19 | 11.20 | 7.78 | 11.6 | O.K |
| 7.50 | 4.23 | 11.46 | | | O.K |
| 10.0 | 4.30 | 11.78 | | | N.O.K |

cantilever beams to resist loads and deflections even if the values of $((f'_c, f_y))$ as a parameter are changed.

- Concerning the loads as a parameter, it was considered the worst distributed load identified locally. Table 5 whose calculations were made on a beam model $(300 \times 600 \times 2,802)$ mm.

The distributed loads should not be increased more than 7.5% in the future. This has been tested on all pass results in Table 3 and proven correct.

- All the published articles and textbooks did not conclude Figure 2 as a simplified roadmap in calculating the various deflections exactly, instead of adopting an approximate method such as finite elements as stated in ref. [9], especially for commonly used geometric sections with $(\rho = 0.005)$ against $\gamma = 1.96$ MPa. Also, Figure 2 shows very attractive, especially for postgraduate and undergraduate students.

3 Conclusion

- The study focused on concluding the optimum dimensions for the reinforced concrete cantilever beams with a rectangular cross section subjected to the uniformly distributed loads commonly used in building construction, excluding the concentrated loads. Due to the significant deflections, it is not easy to select cross sections

of the cantilever beams, especially with a large span. To solve this problem, the authors plot a simplified graph to provide a cross section for the required beam length in less time and effort. The chart does not include deep beams with depths greater than 900 mm, with conditions specified in the ACI code. Also, the current study revealed an important economic aspect. The allowable span lengths are greater than the expected and locally common. Thus, a solution to an old problem has been developed that was not discussed in the published literature.

- The authors strongly recommend using the results in various buildings, provided that no significant concentrated loads are applied along the beams and future uniform distributed loads do not exceed 7.5% used in the current study.
- Since the increase in (ρ) increases the length of the beam, and the designer is restricted to the length adopted by this study, then any increase in (ρ) will be safer even if the values of (f'_c, f_y) are changed.
- Sustained deflections are the most dangerous types of deflections.
- The authors created a simplified algorithm for calculating deflections that are not found in any published article or textbook.
- Using a beam of more than 350 mm in width is not economical.

Funding information: We declare that the manuscript was done depending on the personal effort of the author, and there is no funding effort from any side or organization, as well as no conflict of interest with anyone related to the subject of the manuscript or any competing interest.

Conflict of Interest: The authors state no conflict of interest.

Data availability statement: Most datasets generated and analyzed in this study are in this submitted manuscript. The other datasets are available on reasonable request from the corresponding author with the attached information.

References

- [1] ACI Committee 318. Building code requirements for reinforced concrete (ACI 318-19). Detroit, USA: American Concrete Institute; 2014. p. 398–402.
- [2] Nilson AH, Darwin D, Dolan CW. Design of concrete structures, 14th edn. USA: McGraw-Hill; 2010. p. 767–8.
- [3] Nawy EG. Reinforced concrete a fundamental approach, 6th edn. USA: Pearson Education; 2009. p. 273–311.
- [4] Wang C, Salmon CG, Pincheira JA. Reinforced concrete design, 7th edn. USA: Wiley; 2007. p. 514–43.
- [5] Hassoun MN, Al-Manaseer A. Structural concrete theory and design, 4th edn. USA: Wiley; 2008. p. 190–207.
- [6] McCormac JC, Brown. RH. Design of reinforced concrete, 8th edn. USA: Wiley; 2009. p. 150–72.
- [7] Limbrunner GF, Aghayere AO. Reinforced concrete design, 6th edn. USA: Pearson Education; 2007. p. 216–30.
- [8] Ghamry K. Effect of supports position on the immediate deflection for reinforced concrete beam. In Institute of Research Engineers and Doctors, LLC; 2015. p. 38–42.
- [9] Chaphalkar SP, Subhash NK, Arun MM. Modal analysis of cantilever beam structure using finite element analysis and experimental analysis. Am J Eng Res. 2015;4:178–85.
- [10] Marovic P, Galic M, Putnik G. Deflection Determination of the cantilever with variable circular hollow cross-section. 8th International Congress of Croatian Society of Mechanics, Opatija, Croatia; 2015. p. 1–10. <https://www.researchgate.net/publication/282643743>.
- [11] Gunel MH. Deflections of reinforced concrete beams and columns. Post Graduate Thesis, Middle East Technical University. Ankara, Turkey: Department of Civil Engineering; 1995.
- [12] Oladejo K, Abu R, Bamiro O. Model for deflection analysis in cantilever beam. EJERS, Eur J Eng Res Sci. 2018;3:60–6.
- [13] Ban M. Deflection of the serial RC low-tension supply network pole. Graduate Thesis, University of Split, Faculty of Civil Engineering and Architecture, Split, Croatian, 2008.
- [14] Shariq M, Abbas H, Prasad J. Effect of magnitude of sustained loading on the long-term deflection of RC beams. Archiv Civ Mech Eng. 2019;19:779–91.
- [15] Gilbert RI. Creep and shrinkage induced deflections in RC beams and slabs. USA: ACI Special Publication; Vol. 284S; 2012. p. 1–6.
- [16] Shariq M, Abbas H, Prasad J. Effect of GGBFS on time-dependent deflection of RC beams. Comput Concr. 2017;19:51–8.
- [17] Samra RM. Renewed assessment of creep and shrinkage effects in reinforced concrete beams. ACI Struct J. 1997;94:745–51.
- [18] Ghali A, Azarnejad A. Deflection prediction of members of any concrete strength. ACI Struct J. 1999;96:807–17.
- [19] Rosowsky DV, Stewart MG, Khor EH. Early-age loading and long-term deflections of reinforced concrete beams. ACI Struct J. 2000;97:517–24.
- [20] Prombut P, Anakpotchanakul C. Deflection of composite cantilever beams with a constant I-cross section. IOP Conference Series. UK: Materials Science and Engineering; 2019. p. 1–6.
- [21] Nirmal T, Vimala S. Free vibration analysis of cantilever beam of different materials. Int J Appl Eng Res. 2016;5:612–5.
- [22] Espion B, Halleux P. Long-term deflections of reinforced concrete beams: reconsideration of their variability. ACI Struct J. 1990;87:232–6.
- [23] Tsai S, Kan H. The exact solution of the load-deflection model of a uniformly loaded rectangular cross-section cantilever beam. J Physics D. 41, 2008. p. 1–6. IOP Publishing.

Appendix

Appendix A. Input file

```

[(bh = [(250,375),(250,438),(250.500),(250,563),(250.625
[(300,750),(300,675),(300,600),(300,525),(300,450)1
[(350,875),(350,788),(350,700),(350.613),(350,525)1
[(400,800),(400,700),(400,600)1
[(py = [(0.0034,1.38),(0.004,1.65),(0.005. 1%),(0.006,2.38
import math
fc = 28; Es = 200,000; IDL = 25.65;WLL = I 3.5
for bhl in bh ("##### print ("#####")
print
for b,h in bhl
for p,y in py
lg = (b*pow(h ,3))/12
Mcr = ((0.62*math.sqrt(fc))/(h/2))*1g * 0.00000 I
(Ec = 4,700 *math.sqrt(fc n = Es/Ec
d = h-60 As = p*b*d
XI = ((-n*As)+math.sqrt((n*As)**2-4*(b/2)*(-n*As*d)))/b
X2 = ((-n*As)-math .sqrt((n*As)**2-4*(b/2)*(-n*As*d)))/b (X = max(X1,X2
if X>0 Icr = (b*pow(X,3)/3)+n*As*(d-X)**2 self_wcight = 25*b*h*O .00000 I WDL = self_weight+IDL W = WDLHVLL
(L = math.sqrt(2*y*b*(d**2)/W Ma = (WDL *(L**2)/2)*0.00000 I
Ie = pow((Mcr/Ma),3)*1g+( I-pow((Mcr/Ma),3))*1cr (delte_DL = WDL*pow(L,4)/(8*Ec*lc Ma2 = ((WDL+WLL)*(L**2)/2)
*0.00000I
Ie2 = pow((Mcr/Ma2) ,3)*Jg+( I -pow((Mcr/Ma2),3))*1cr (delte_DL_LL = (WDL+WLL)*pow(L,4)/(8*Ec*Ie2 deflection#
delta i LL = delte DL LL-delte DL (pl = 0.002*b*h/(b*d -
(lcmbda = 1.4/(I+50*pl delta_cr_sh = lembda*dcltc_DL delta T = dclta i LL+dclta er sh
print(b,h ,ps,L,dclta_C.LL,dclta_T.sep = "\t")

```

Appendix B. Output file

| b (mm) | h (mm) | p | y | L (mm) | δ_{i_LL} (mm) | δ_{T_LL} (mm) |
|----------|----------|--------|------|--------------|-----------------------|-----------------------|
| 250 | 375 | 0.0034 | 1.38 | 1,284.528535 | 1.204772808 | 1.889216315 |
| 250 | 375 | 0.0040 | 1.65 | 1,404.579046 | 1.827000915 | 3.224234404 |
| 250 | 375 | 0.0050 | 1.96 | 1,530.848626 | 2.255624256 | 4.704488116 |
| 250 | 375 | 0.0060 | 2.38 | 1,686.913025 | 2.721597045 | 6.825838556 |
| 250 | 438 | 0.0034 | 1.38 | 1,534.172256 | 1.557049476 | 2.561536276 |
| 250 | 438 | 0.0040 | 1.65 | 1,677.554173 | 2.228283574 | 4.199480124 |
| 250 | 438 | 0.0050 | 1.96 | 1,828.363814 | 2.629206231 | 5.920507015 |
| 250 | 438 | 0.0060 | 2.38 | 2,014.758794 | 3.113463796 | 8.383454045 |
| 250 | 500 | 0.0034 | 1.38 | 1,777.605616 | 1.877419335 | 3.219220743 |
| 250 | 500 | 0.0040 | 1.65 | 1,943.738526 | 2.581116647 | 5.132813167 |
| 250 | 500 | 0.0050 | 1.96 | 2,118.477746 | 2.963310207 | 7.074662906 |
| 250 | 500 | 0.0060 | 2.38 | 2,334.448777 | 3.481715347 | 9.864884763 |
| 250 | 563 | 0.0034 | 1.38 | 2,022.728391 | 2.179406299 | 3.878081765 |
| 250 | 563 | 0.0040 | 1.65 | 2,211.770184 | 2.908877273 | 6.056306431 |

| | | | | | | |
|-----|-----|--------|------|--------------|-------------|-------------|
| 250 | 563 | 0.0050 | 1.96 | 2,410.605054 | 3.280388006 | 8.21283743 |
| 250 | 563 | 0.0060 | 2.38 | 2,656.357393 | 3.842227813 | 11.32941511 |
| 250 | 625 | 0.0034 | 1.38 | 2,261.803606 | 2.456848024 | 4.515493355 |
| 250 | 625 | 0.0040 | 1.65 | 2,473.189084 | 3.208436785 | 6.943120486 |
| 250 | 625 | 0.0050 | 1.96 | 2,695.525127 | 3.57580832 | 9.304360088 |
| 250 | 625 | 0.0060 | 2.38 | 2,970.324022 | 4.18477208 | 12.73693728 |
| 300 | 450 | 0.0034 | 1.38 | 1,720.907845 | 1.899491023 | 3.189672859 |
| 300 | 450 | 0.0040 | 1.65 | 1,881.741848 | 2.689818385 | 5.19741351 |
| 300 | 450 | 0.0050 | 1.96 | 2,050.907658 | 3.149179882 | 7.289701599 |
| 300 | 450 | 0.0060 | 2.38 | 2,259.990167 | 3.719227507 | 10.28437955 |
| 300 | 525 | 0.0034 | 1.38 | 2,038.414374 | 2.333452058 | 4.122412669 |
| 300 | 525 | 0.0040 | 1.65 | 2,228.92216 | 3.161096716 | 6.514015756 |
| 300 | 525 | 0.0050 | 1.96 | 2,429.298967 | 3.595194997 | 8.913498439 |
| 300 | 525 | 0.0060 | 2.38 | 2,676.957082 | 4.215627041 | 12.36761068 |
| 300 | 600 | 0.0034 | 1.38 | 2,351.88891 | 2.727181776 | 5.034615173 |
| 300 | 600 | 0.0040 | 1.65 | 2,571.693653 | 3.583057672 | 7.785721304 |
| 300 | 600 | 0.0050 | 1.96 | 2,802.885112 | 4.00502623 | 10.4772138 |
| 300 | 600 | 0.0060 | 2.38 | 3,088.628962 | 4.686845969 | 14.37947906 |
| 300 | 675 | 0.0034 | 1.38 | 2,661.446545 | 3.0876788 | 5.92449322 |
| 300 | 675 | 0.0040 | 1.65 | 2,910.182177 | 3.968212988 | 9.017677454 |
| 300 | 675 | 0.0050 | 1.96 | 3,171.803253 | 4.387258686 | 11.99057637 |
| 300 | 675 | 0.0060 | 2.38 | 3,495.156955 | 5.134825763 | 16.33102449 |
| 300 | 750 | 0.0034 | 1.38 | 2,967.197551 | 3.420295323 | 6.792258796 |
| 300 | 750 | 0.0040 | 1.65 | 3,244.50831 | 4.323955165 | 10.21396181 |
| 300 | 750 | 0.0050 | 1.96 | 3,536.184811 | 4.746234304 | 13.45978324 |
| 300 | 750 | 0.0060 | 2.38 | 3,896.685874 | 5.560589567 | 18.22890816 |
| 350 | 525 | 0.0034 | 1.38 | 2,185.161352 | 2.647921466 | 4.745996234 |
| 350 | 525 | 0.0040 | 1.65 | 2,389.383936 | 3.580501887 | 7.499118209 |
| 350 | 525 | 0.0050 | 1.96 | 2,604.18602 | 4.066801826 | 10.25975533 |
| 350 | 525 | 0.0060 | 2.38 | 2,869.673227 | 4.766943236 | 14.23240888 |
| 350 | 613 | 0.0034 | 1.38 | 2,576.123049 | 3.153073087 | 5.963814076 |
| 350 | 613 | 0.0040 | 1.65 | 2,816.884449 | 4.116546697 | 9.19342417 |
| 350 | 613 | 0.0050 | 1.96 | 3,070.118197 | 4.585419233 | 12.33972662 |
| 350 | 613 | 0.0060 | 2.38 | 3,383.10548 | 5.364770151 | 16.90585678 |
| 350 | 700 | 0.0034 | 1.38 | 2,956.237404 | 3.599176564 | 7.128713119 |
| 350 | 700 | 0.0040 | 1.65 | 3,232.523841 | 4.588461835 | 10.80164112 |
| 350 | 700 | 0.0050 | 1.96 | 3,523.122956 | 5.053681076 | 14.31195702 |
| 350 | 700 | 0.0060 | 2.38 | 3,882.292411 | 5.916382436 | 19.44735853 |
| 350 | 788 | 0.0034 | 1.38 | 3,334.484507 | 4.006319426 | 8.26857538 |
| 350 | 788 | 0.0040 | 1.65 | 3,646.121468 | 5.019921686 | 12.36836927 |
| 350 | 788 | 0.0050 | 1.96 | 3,973.902398 | 5.489907668 | 16.23294524 |
| 350 | 788 | 0.0060 | 2.38 | 4,379.027164 | 6.436849677 | 21.92741333 |
| 350 | 875 | 0.0034 | 1.38 | 3,702.493016 | 4.372149225 | 9.359433503 |
| 350 | 875 | 0.0040 | 1.65 | 4,048.523615 | 5.408836445 | 13.86360523 |
| 350 | 875 | 0.0050 | 1.96 | 4,412.479904 | 5.888618307 | 18.06639311 |
| 350 | 875 | 0.0060 | 2.38 | 4,862.316036 | 6.916459073 | 24.29757779 |
| 400 | 600 | 0.0034 | 1.38 | 2,670.234601 | 3.413739737 | 6.516244229 |
| 400 | 600 | 0.0040 | 1.65 | 2,919.791555 | 4.467862884 | 10.07529493 |
| 400 | 600 | 0.0050 | 1.96 | 3,182.2765 | 4.98213654 | 13.55243852 |
| 400 | 600 | 0.0060 | 2.38 | 3,506.69791 | 5.828305797 | 18.59110858 |
| 400 | 700 | 0.0034 | 1.38 | 3,130.24736 | 3.966187244 | 8.010752646 |

| | | | | | | |
|-----|-----|--------|------|--------------|-------------|-------------|
| 400 | 700 | 0.0040 | 1.65 | 3,422.796561 | 5.046467123 | 12.13636773 |
| 400 | 700 | 0.0050 | 1.96 | 3,730.500912 | 5.552493174 | 16.0761737 |
| 400 | 700 | 0.0060 | 2.38 | 4,110.811789 | 6.500408425 | 21.83899311 |
| 400 | 800 | 0.0034 | 1.38 | 3,580.761603 | 4.450992282 | 9.443540174 |
| 400 | 800 | 0.0040 | 1.65 | 3,915.415329 | 5.555043299 | 14.10193199 |
| 400 | 800 | 0.0050 | 1.96 | 4,267.40538 | 6.065308054 | 18.48226539 |
| 400 | 800 | 0.0060 | 2.38 | 4,702.451697 | 7.114153209 | 24.94214265 |

Appendix C. Example

Take any passing result from Table 3. Let it be (300 × 600 × 2802 mm as well as an algorithm parameter; $f'_c = 28$ MPa, $f_y = 414$ MPa, IDL = 25.65 kN/m, and $W_{LL} = 13.5$ kN/m. Self-weight = 25(300)(600) ×

$$10^{-6}$$

$$= 4.5 \text{ kN/m}$$

$$W_{DL}$$

$$= 4.5 + 25.65 = 30.15 \text{ kN/m,}$$

Factored ultimate loads are; $W_u = 1.2(30.15) + 1.6(13.5) = 57.78 \text{ kN/m}$

$$M_u = \frac{W_u \ell^2}{2} = \frac{(57.78)(2802)^2}{2} \times 10^{-6} = 227 \text{ kN m}$$

$$\rho = \frac{f'_c}{1.18f_y} \left[1 - \sqrt{1 - \frac{2.36M_u}{0.9bd^2f'_c}} \right] = \frac{28}{1.18(414)} \left[1 - \sqrt{1 - \frac{2.36(227) \times 10^6}{0.9(300)(600 - 60)^2(28)}} \right]. \quad (A1)$$

$$\rho = 0.0074 > 0.005$$

Provided reinforcement ratio remains greater than 0.005 when any value of $\left(\frac{f_y}{f'_c}\right)$ in Figure 1 is substituted into equation (A1).